Available online at www.sciencedirect.com
SCIENCE DIRECT®
Pattern Recognition Letters 27 (2006) 937–946
Pattern Recognition Letters
www.elsevier.com/locate/patrec

Benefit of the angular texture signature for the separation of parking lots and roads on high resolution multi-spectral imagery

Qiaoping Zhang *, Isabelle Couloigner

Department of Geomatics Engineering, University of Calgary, 2500 University Drive N.W., Calgary, Alberta, Canada T2N 1N4

Received 13 May 2005; received in revised form 22 November 2005
Available online 2 February 2006

Communicated by Prof. H.H.S. Ip

Abstract

The misclassification of roads and parking lots is one of the major difficulties in automating road network extraction from high resolution remotely-sensed imagery, especially in urban areas. This paper proposes a new integrated approach to road identification on high resolution multi-spectral imagery. The input images are first segmented using a traditional *k*-means clustering on normalized digital numbers. The road cluster is then automatically identified using a fuzzy logic classifier. A number of shape descriptors of angular texture signature are introduced for a road class refinement, i.e. to separate the roads from the parking lots that have been misclassified as roads. Intensive experiments have shown that the proposed methodology is effective in automating the separation of roads from parking lots on high resolution multi-spectral imagery.

Keywords: Road extraction; Multi-spectral imagery; Image segmentation; Shape descriptor; Texture

1. Introduction

During the last two decades, substantial work has been completed for automatic road extraction from remotely-sensed imagery in the photogrammetric and computer vision communities. Accordingly, dozens of different strategies or algorithms are proposed in the existing literature (Mena, 2003; Baltsavias, 2004; Mena and Malpica, 2005). However, there is little research conducted on road network extraction from multi-spectral imagery (MSI) (Doucette et al., 2001, 2004). This situation is now changing with the increasing availability of high spatial resolution MSI. At the same time, MSI has a great advantage over panchromatic or other grey-level imagery as it enhances the capability to discriminate road surface material from most of the other types of landscape materials. For example, the multi-spectral data usually includes a NIR band that is a powerful discriminator of vegetation and man-made surfaces. This could be very helpful in a road identification step. With the emergence of new advanced data fusion technologies, it is now even possible to extract road networks from pan-sharpened MSI in urban areas (e.g. Zhang and Wang, 2004).

The task of road extraction addresses two issues: (1) identification and (2) delineation (Doucette et al., 2001). A semi-automated algorithm relies on user-provided cues (e.g. seed points or initial directions) to identify the approximate location of a road. By contrast, fully automated methods attempt to integrate aspects of identification and delineation to achieve true operational autonomy. Most of the existing road extraction methods for MSI rely heavily on automatic and reliable classification of road surfaces (e.g. Doucette et al., 1999, 2001; Amini et al., 2002; Song and Civco, 2004). Unfortunately, the classification accuracy of roads is far from satisfactory whether a supervised classification method or an unsupervised method is used.

* Corresponding author. Tel.: +1 403 2208038; fax: +1 403 2841980.
E-mail addresses: qzhang@geomatics.ucalgary.ca, qzhang_geo@yahoo.ca (Q. Zhang), couloigner@geomatics.ucalgary.ca (I. Couloigner).

0167-8655/$ - see front matter © 2005 Elsevier B.V. All rights reserved.
doi:10.1016/j.patrec.2005.12.003

The main difficulty lies in the high misclassification between roads and parking lots, and between roads and some building roof materials.

Quackenbush (2004) has pointed out that a number of articles specifically take advantage of the multi-spectral nature of sensors such as Landsat TM, SPOT and Ikonos to extract road information. However, in most cases, even with hyperspectral datasets, the spectral information alone was not sufficient to define roads and the classification was one component of a multistage process. Gardner et al. (2001) found that classification of roads using AVIRIS imagery was challenging because of the similarities of construction materials in roads and roofs. They found that following the classification with the spatial pattern recognition technique of a Q-tree filter improved the result.

Road and parking lot surfaces often use the same construction materials and thus will have similar spectral signatures, which make it very difficult to automatically separate them from a remotely-sensed image. Introducing other information (e.g. height data from Lidar, clues from detected vehicles) does not measurably improve the situation due to the fact that roads and parking lots are usually at the same level and both will usually be occupied by vehicles. Research on the classification of roads and parking lots is quite recent partly due to the fact that road network extraction in urban areas becomes more feasible with the availability of high resolution remotely-sensed imagery.

In (Hu et al., 2004), the vehicle clue is used to verify a parking area in combination with a morphologic operation, which is applied to the classified image to detect big open areas. The vehicles are extracted by a pixel based classification method. It is assumed that a region with a nearly squared shape and large area has a high possibility of being a parking lot. The output from this step is used to improve the detected road segments from a Hough transform. Although the test results from 0.5 m resolution color ortho-imagery with Lidar data are quite good, there is no detail available on how to identify the large open areas using the morphologic operation. On the other hand, their research confirms our belief that although introducing Lidar data helps in building extraction; it helps little in road network extraction because it does not improve our ability to separate parking lots from roads.

Based on image classification results from pan-sharpened imagery, Zhang and Wang (2004) apply a segment filtering algorithm to deal with large parking lots and buildings which are misclassified as road networks. Basically, a directional texture detector is developed to distinguish different types of objects according to their textures in different directions. The directional texture detector measures the pixel grey value variance along the central lines in each of four directions (horizontal and vertical) of an operation window. If all the variances in the four directions are smaller than a certain value, it can be concluded that the object within this window is homogeneous and can be considered as a non-road object. This object can then be removed. The work demonstrates that it is possible to extract urban objects from pan-sharpened imagery. However, the separation of parking lots and buildings from road networks is not satisfactory. There are many artifacts introduced by the directional texture detector.

The directional texture measure is also known as the angular texture signature (ATS). It was used by Haverkamp (2002) and Gibson (2003) for finding road networks in Ikonos satellite imagery. The texture measure that they used as a road detector had two components: the degree of the pixel (i.e. the number of the strong local minima in the angular texture signature) and the direction of the minimum.

Song and Civco (2004) used two shape measures, namely smoothness and compactness, to further reduce the misclassification between roads and other spectrally similar objects from a support vector machine (SVM) classifier. The two shape measures were derived by the commercial software eCognition©. Experiments on Ikonos MS imagery showed that the SVM classifier has a slightly better performance than the traditional maximum likelihood classifier in terms of overall classification accuracy. By combining the spectral information and shape measures they were able to remove most of the false-road objects in the road group.

Doucette et al. (1999) performed a principal component analysis on hyperspectral digital imagery collection experiment (HYDICE) imagery, and then used a maximum likelihood classification to generate a classified layer. This classified layer was combined with coarse GIS data in a neural network in order to extract linear features. The GIS data provided approximate location information for the extraction, speeding up convergence while minimizing user input. A self-organized road map (SORM) was developed by Doucette et al. (2001) for extracting road networks from classified imagery. Doucette et al. (2004) presents a novel methodology for fully automated road centerline extraction that exploits the spectral content from high resolution multi-spectral images. Preliminary detection of candidate road centerline components is performed with anti-parallel-edge centerline extraction (ACE). This is followed by constructing a road vector topology with a fuzzy grouping model that links nodes from a self-organized mapping of the ACE components. Following topology construction, a self-supervised road classification (SSRC) feedback loop is implemented to automate the process of training sample selection and refinement for a road class, as well as deriving practical spectral definitions for non-road classes. SSRC demonstrates a potential to provide dramatic improvement in road extraction results by exploiting the spectral content. Road centerline extraction results are presented for three 1 m color infrared suburban scenes which show significant improvement following SSRC.

In (Gao and Wu, 2004), the Ikonos MS image is first classified into road and non-road classes. The road class is refined by removing the noisy pixels such as the building

pixels by a spatial filter based on the assumption that all the small size components are not real road pixels. The road segments are then joined and thinned to form a road network.

In (Tarku et al., 2004), the coarse road class is obtained by thresholding the original panchromatic image. Refinement is achieved by removing the false road pixels based on a connected component analysis. Small components, dense components, and irregular components are less likely to be a road-based component. They are identified and removed from the road class.

In this paper, we propose a new approach to effectively identify the parking lots/buildings from the road cluster resulting from a spectral clustering. The new approach is based on a number of shape descriptors of the angular texture signature in combination with a fuzzy classifier.

This paper is organized into five sections. First, a brief description of the framework we used for the road identification on multi-spectral imagery is given in Section 2. Then the three main steps, image segmentation using spectral clustering, automatic road cluster identification, and road class refinement, are discussed in detail in Sections 3–5, respectively. Section 6 summarizes our research and concludes the paper.

2. Overview

The proposed approach starts with an image segmentation using the *k*-means algorithm (Fig. 1). This step mainly concerns the exploitation of the spectral information as much as is possible for feature extraction. The road cluster is then identified automatically using a fuzzy classifier based on a set of predefined membership functions for road surfaces. These membership functions are established based on the general spectral signature of road pavement materials and the corresponding normalized digital numbers on each multi-spectral band. Finally, we define a number of shape descriptors for the angular texture signature. These measures are used to reduce the misclassifications between the roads and parking lots/buildings. The whole process is unsupervised and fully automated.

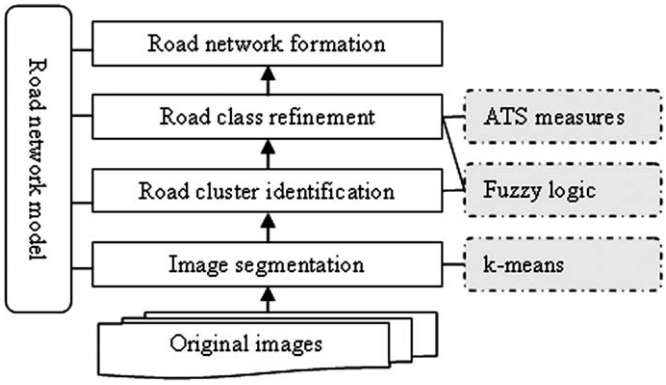

Fig. 1. Overview of road identification on multi-spectral imagery.

3. Image segmentation

Image segmentation is the division of an image into meaningful structures, called regions or segments (Heijden, 1994). The partitioning is meaningful if and only if a correspondence is known to exist between segments and parts of the object being "imaged". There are a number of methods for image segmentation, ranging from edge-based approaches to region-based algorithms (Gonzalez and Woods, 2002). However, most of the algorithms mainly work on grey-level imagery. For multi-spectral imagery, spectral clustering algorithms are often used. These include *k*-means, ISODATA, mean shift (Comaniciu and Meer, 2002) classifiers and so on. In our research, the *k*-means algorithm is applied because of its simplicity and efficiency. All the four bands of an Ikonos image are used in the spectral clustering. Although any number from five to seven works well for most of our test images, six is selected as the number of clusters for all the cases in this research. To achieve a better clustering quality, it is recommended that the number of clusters be optimized using the approaches presented in (Doucette et al., 2001). Fig. 2 shows a typical output of the *k*-means algorithm from our Ikonos MS imagery.

From Fig. 2, we can see that the classification process is able to find the road cluster from other land coverage clusters on multi-spectral imagery. The major problem, however, is the huge misclassification between the roads and parking lots/buildings, which motivates us to find a way to separate the roads from the parking lots/building in the road cluster.

4. Automatic road cluster identification

To automate the whole process, we need to find a way to automatically identify the road cluster in the classified image. Thanks to the discriminating capability of the multi-spectral imagery, the road cluster does have its own signature in the final means of each cluster.

Generally speaking, the road surface has relatively higher reflectance in the blue, green, and red bands, while it has a relatively lower reflectance in the near infrared band. The problem is how to model these spectral signatures mathematically. Several methods have been tried in our research. We found out that the direct digital number (DN) of the final means is not reliable because this DN will vary with different scenes. The normalized DN of the final means by min–max normalization is better, but the normalized DN of the final means by mean–standard deviation normalization gives us the best results. In our research, the mean–standard deviation normalization (Eq. (1)) is applied for each band in the classified clusters and the final means are used to automatically find the road cluster.

$$\mathrm{DN}_1 = \frac{\mathrm{DN}_0 - \mathrm{mean}_0}{\sigma_0}, \tag{1}$$

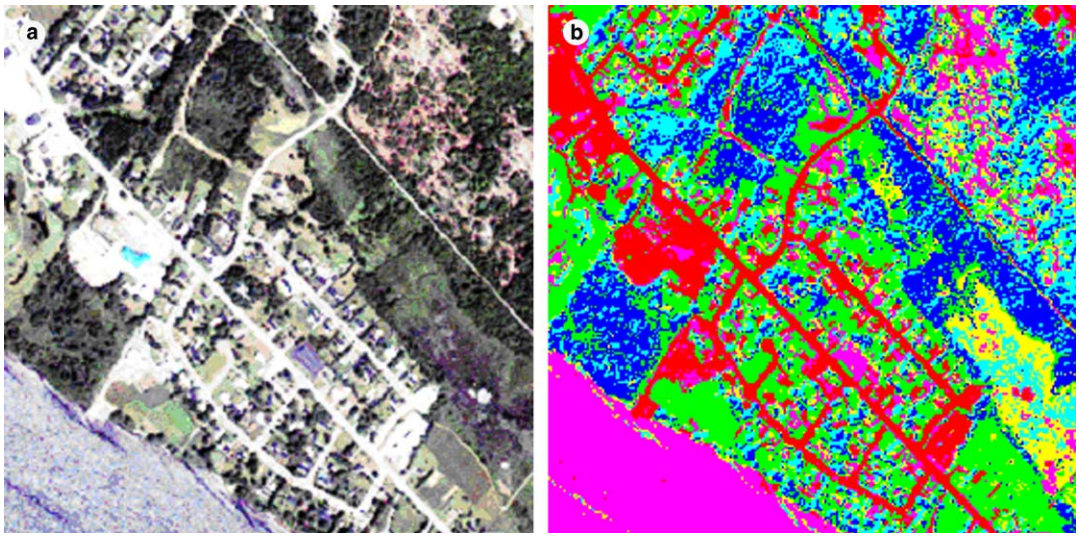

Fig. 2. A typical output of the *k*-means algorithm from Ikonos MS imagery: (a) original true color composite ortho-image; (b) segmented image with the road cluster shown in red.

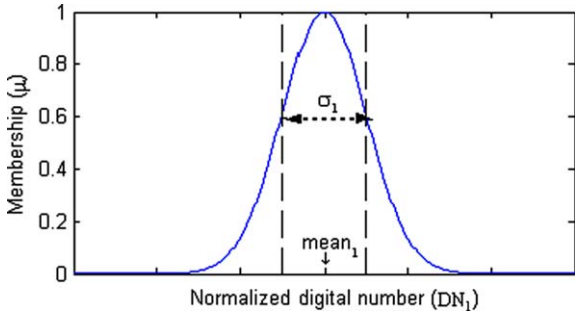

Fig. 3. A plot of the Gaussian membership function.

where DN_0 and DN_1 are the original and normalized digital number respectively, $mean_0$ and σ_0 are the mean and standard deviation of the original digital number for each band.

A fuzzy logic classification is then applied to identify the road cluster. We used the Gaussian membership functions for all four bands (Eq. (2) and Fig. 3).

$$\mu(DN_1) = \exp\left(-\frac{(DN_1 - mean_1)^2}{2\sigma_1^2}\right), \quad (2)$$

where DN_1 is the normalized digital number of each band of the final cluster, $mean_1$ and σ_1 are the mean and standard deviation of the normalized digital number for each band.

The corresponding means and standard deviations are listed in Table 1. The cluster which has the highest combined road membership is labeled as the road cluster. The combined road membership is the multiplication of the road memberships from each band. The identified road cluster in Fig. 2(b) is the one shown in red.[1]

Table 1
The parameters used in the Gaussian membership functions for automatic road cluster identification

Band	Blue	Green	Red	NIR
Mean	1.50	1.50	1.50	−0.50
Std	0.25	0.25	0.25	0.25

A number of different Ikonos MS ortho-images have been tested. The results are identical to human visual inspection ones and are quite robust. The tested images were captured in different years and are covering different areas.

It is worthy to mention that the proposed approach can be directly applied to Quickbird MS imagery without any changes. Fig. 4 shows the result from one of our Quickbird test images.

5. Road class refinement

As mentioned above, the road cluster resulting from the classification is a mix of roads, parking lots and buildings. Further refinement is needed to remove the non-road regions before we can perform a road network formation. In this research, the road class refinement is achieved by an advanced application of the angular texture signature and its derived shape descriptors. The road network formation will be our future work and is not covered in this paper.

5.1. Basic angular texture signature

A texture measure is described in (Haverkamp, 2002; Gibson, 2003) and defined as follows. At each pixel p of a panchromatic image, $T(\alpha, w, p)$ is defined as the variance from the mean for a rectangular set of pixels of width w around the point p whose principal axis lies at an angle

[1] For interpretation of colour in Figs. 2, 4, 6, 7, 11–13 the reader is referred to the web version of this article.

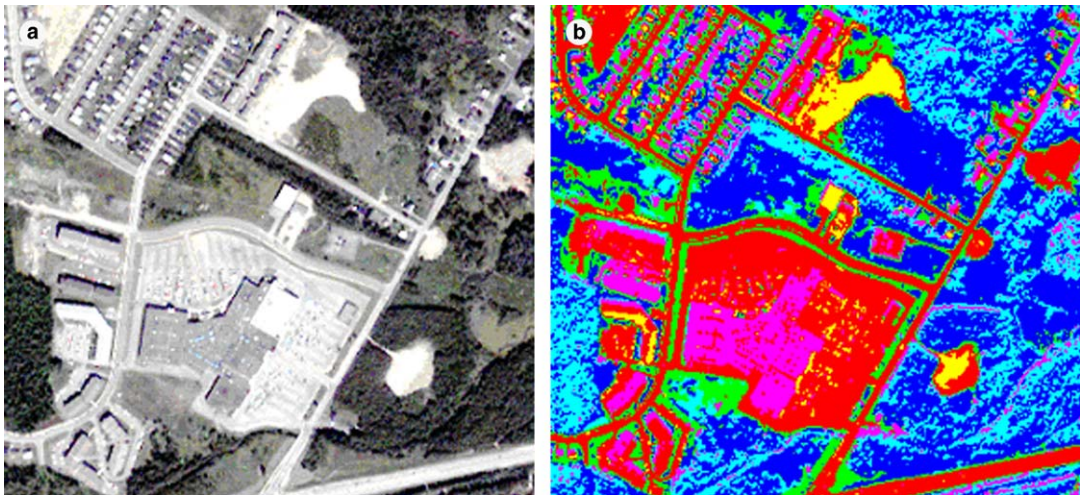

Fig. 4. A typical output of the k-means algorithm from a Quickbird MS image (a) original true color composite ortho-image; (b) segmented image with the identified road cluster shown as red.

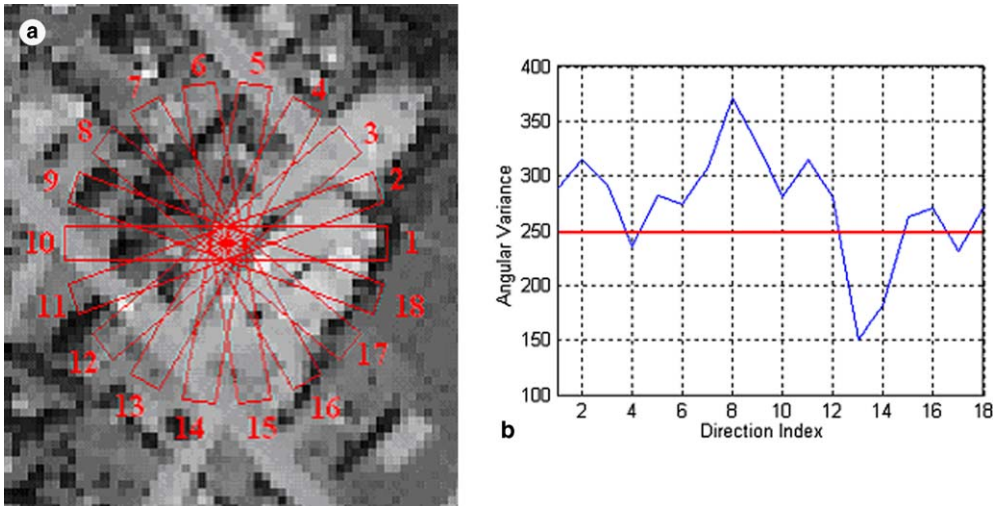

Fig. 5. Texture is computed over a set of rectangular regions about pixel (a) and the graph of the angular texture signature for a single pixel (b). The image used is a subset of an Ikonos MS-red image. For illustration purpose, the size of the rectangular regions is set to 5 by 20 pixels (after (Gibson, 2003)).

of α from the horizontal. This measure is computed for a set of angles $\alpha_0, \ldots, \alpha_n$. Fig. 5(a) shows the templates for a single point. At the point p, the angular texture signature is defined as the set of values $\{T(\alpha_0, w, p), T(\alpha_1, w, p), \ldots, T(\alpha_n, w, p)\}$.

The graph of an angular texture signature for a single point p is shown in Fig. 5(b). The local minima on this graph correspond to the most likely directions of the road at p (e.g. directions 4 and 13 in Fig. 5). At each pixel p, the number k and location of the strong local minima are computed from the angular texture signature. For example, the signature shown in Fig. 5(b) has three minima that are significant (i.e. less than 250 in this case). We refer to the number k of minima as the degree of the pixel. The texture measures that are usually used in road detection are: the degree of the pixel and the direction of the minimum.

To simplify the computation, we define the ATS based only on the road pixels. We compute the ATS based on the binary image of our road cluster, where the road pixels are white (pixel value = 1) and their surrounding pixels are black (pixel value = 0). Furthermore, instead of calculating the variance, we use the mean value only. The mean value is equal to the number of road pixels divided by the total number of pixels within the rectangular region. This normalizes the ATS values to the range of $[0, 1]$. Because we are using a binary image, we define the number of maximum as the ATS-degree of the pixel and the direction of the maximum as the ATS-direction. Fig. 6 illustrates the ATS-degree and ATS-direction of the image shown in Fig. 2. The number of directions we used is 18 and the size of the rectangular region is 5 by 10 pixels in this case. The size of the rectangular region is determined based on the

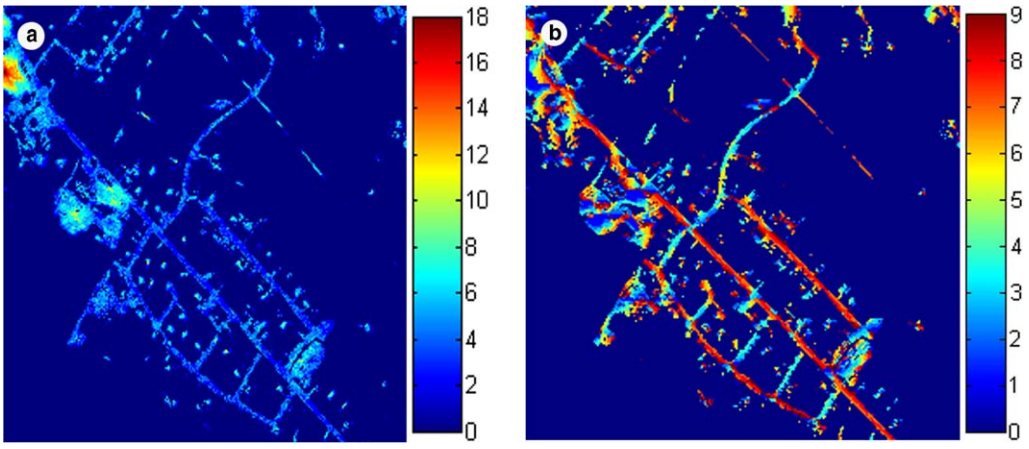

Fig. 6. ATS-degree (a) and direction (b) of the image shown in Fig. 2. In (b) the direction indexes are the same as in Fig. 5(a).

typical road width in the scene. The basic rule is that the width of the rectangular region should be less or equal to the typical road width, and the length should be at least twice the width of the typical road. In our research, we use 5 by 10 pixels for IKONOS MS imagery and 5 by 20 pixels for Quickbird MS imagery.

As we can see from Fig. 6, the ATS-degree does give us a sense of the location of the parking lots (e.g. red area at the upper-left corner). However, the ATS-degree and ATS-direction are very sensitive to the neighboring pixels. The resulting images are very "noisy" and make them very difficult to threshold. We developed some shape descriptors

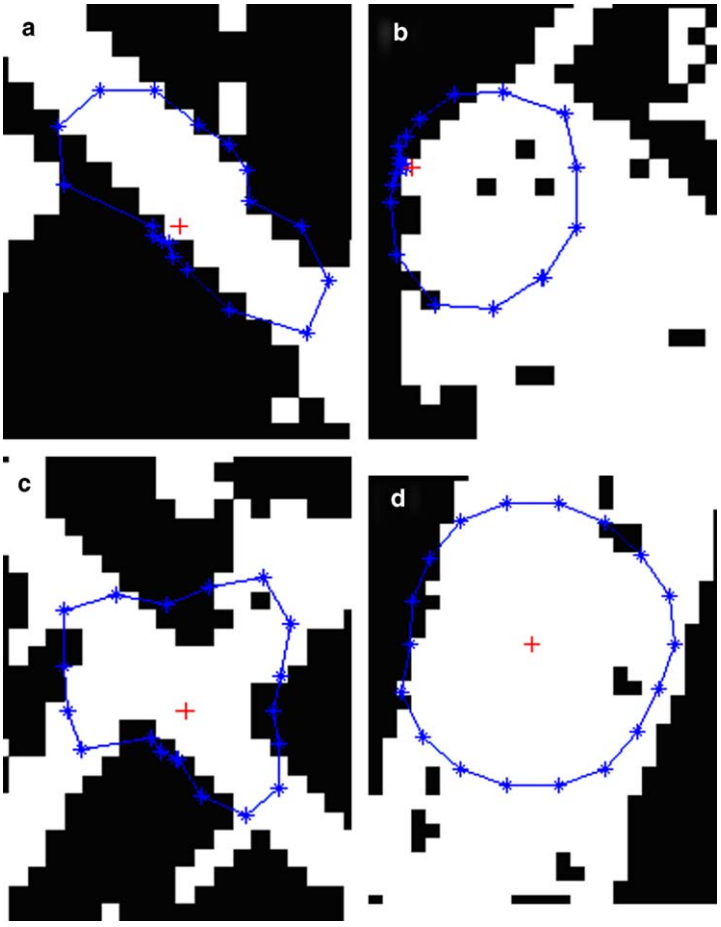

Fig. 7. Angular texture signature for (a) a pixel on a road; (b) a pixel near the corner of a parking lot; (c) a pixel near a T-road junction; (d) a pixel in a parking lot.

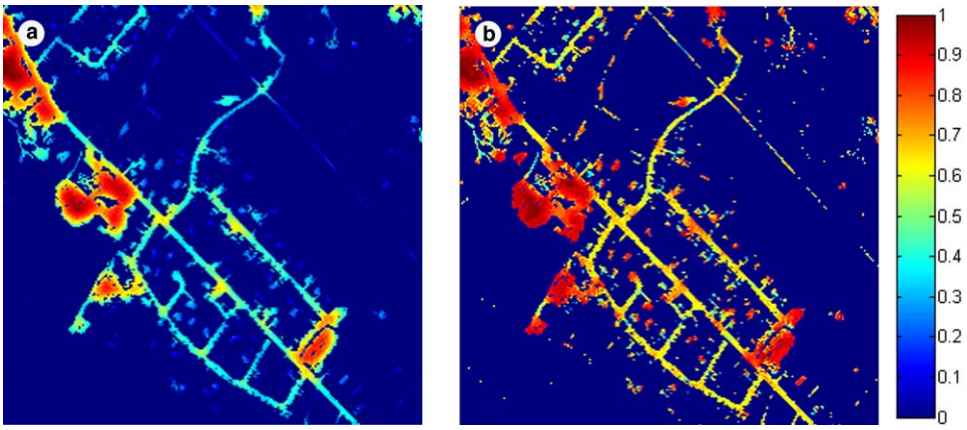

Fig. 8. ATS-mean (a) and ATS-compactness (b) of the image shown in Fig. 2.

based on ATS, which are more suitable for identifying parking lots from roads.

5.2. Shape descriptors of angular texture signature

When we take a closer look at the ATS of each pixel, we can find some interesting links between the shape of the ATS polygon and the corresponding pixel types. To form the ATS polygon, instead of plotting the ATS values for each direction along a horizontal line, we plot the ATS values around the pixel under consideration with the corresponding directions and link the last point to the first point. The resulting polygon is called the ATS polygon. Fig. 7 shows the calculated ATS for some interesting pixels with the ATS polygons shown in blue. The pixels under consideration are marked with a red cross. For illustration purpose, all the ATS polygons are enlarged by a factor of the length of the rectangular region, i.e. 10 pixels in this case.

We define the following shape descriptors for ATS:

(1) *Mean:* The mean of the ATS is defined as the mean ATS value for all directions (Eq. (3)). It tells us the average percentage of object pixels surrounding the current pixel within the rectangular region. A pixel on a parking lot or building will have a larger ATS-mean than a road pixel. Fig. 8(a) confirms this assumption.

$$\mathrm{ATS}_{\mathrm{mean}} = \frac{1}{n}\sum_{i=1}^{n}\mathrm{ATS}(i), \tag{3}$$

where n is the number of directions.

(2) *Compactness:* The compactness of the ATS is defined as the compactness of the ATS polygon using Eq. (4). It tells us whether the shape of the ATS polygon looks like a circle. A circle-like ATS polygon usually means that a pixel is on a parking lot or a building (Fig. 7(b) and (d)). It can be seen clearly in Fig. 8(b) that the parking lots and buildings have very large compactness values.

$$\mathrm{ATS}_{\mathrm{compactness}} = \frac{4\cdot\pi\cdot A}{P^2}, \tag{4}$$

where A and P are the area and perimeter of the ATS polygon, respectively.

(3) *Eccentricity:* The eccentricity of the ATS is defined as the discrepancy between the origin point of the ATS polygon (i.e. the point under consideration) and the centroid of the ATS polygon (Eq. (5)). If a pixel lies at the corner of a

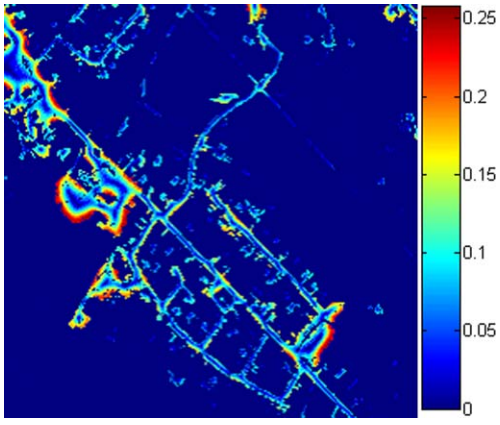

Fig. 9. ATS-eccentricity of the image shown in Fig. 2.

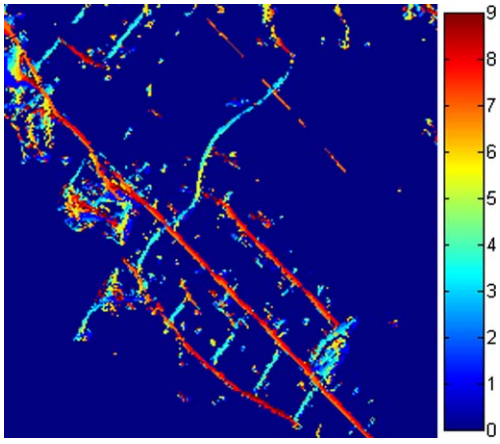

Fig. 10. ATS-direction of the image shown in Fig. 2. The direction indexes are the same as in Fig. 5(a).

parking lot or building, the eccentricity will be relatively larger than those closer to the center of the feature (Fig. 9). Experiments have shown that the boundary problem could be reduced greatly by introducing the ATS-eccentricity in the detection of parking lots.

$$\mathrm{ATS}_{\mathrm{eccentricity}} = \sqrt{(x_c - x_0)^2 + (y_c - y_0)^2}, \quad (5)$$

where (x_c, y_c) is the centroid of the ATS polygon and (x_0, y_0) the origin point.

(4) *Direction:* The direction of the ATS is redefined as the direction of the symmetric maximum direction, i.e. if the direction n_i gives a maximum and one of the directions (n_{i-1}, n_i, n_{i+1}) is also a local maximum then the direction n_i will be identified as a symmetric maximum direction and will be used as the direction of the ATS. Among all the symmetric maximum directions we select the one that has the largest combination ATS value (i.e. the sum of the direction pairs) as the ATS-direction of this pixel. The new defined ATS-direction is more meaningful than the original one and more useful in the road network formation process. This is evident in Fig. 10, which shows the coded ATS-direction of the test image. The directions of the road pixels are more consistent comparing with the basic ATS-direction shown in Fig. 6(b).

5.3. Road class refinement using the angular texture signature

Again, we use a fuzzy logic classification to separate the roads and parking lots/buildings based on the ATS shape descriptors defined in the previous section.

The parameters used in this step are listed in Table 2. Note that, based on our previous definitions, the three shape descriptors (ATS-mean, ATS-compactness, and ATS-eccentricity) have values in the range of $[0, 1]$. Fig. 11(a) shows the road membership for each pixel.

Table 2
The parameters used in the Gaussian membership functions for the road class refinement

	ATS	ATS-compactness	ATS-eccentricity
Mean	0.25	0.40	0.05
Std	0.20	0.20	0.05

Fig. 11(b) is the result after thresholding Fig. 11(a) at a membership of 0.1. Fig. 12 is the output for another Ikonos MS test image. Fig. 13 is the result from the Quickbird MS test image shown in Fig. 4.

From Figs. 11–13, we can see clearly that the proposed approach is able to identify the parking lots/buildings effectively. Most of the parking lots have been successfully identified and completely separated from the road networks.

To evaluate the classification results, we manually identified the non-road pixels (parking lots, buildings, crops, etc.) from the road cluster images and used this information as the reference. Table 3 shows the overall classification accuracy from our four test images. The kappa statistics were calculated using the approach described in (Congalton and Green, 1999). As we can see from Table 3, the four p-values are less than 0.00001 suggesting the proposed approach classifies almost certainly better than random chance.

Although the overall classification accuracy is satisfactory, we do have concerns about the relatively high false alarm rate, that is, classifying real road pixels into non-road pixels, because this will harm the road network topology. As we can see from Figs. 11–13, most of this type of misclassification occurs on the roads that are closely adjacent to parking lots/buildings, or are part of road intersections. One of the possible solutions to these two situations is to integrate the information from the ATS-direction. It is evident that the ATS-direction for roads (even at the road intersections) gives a consistent clue for road formation.

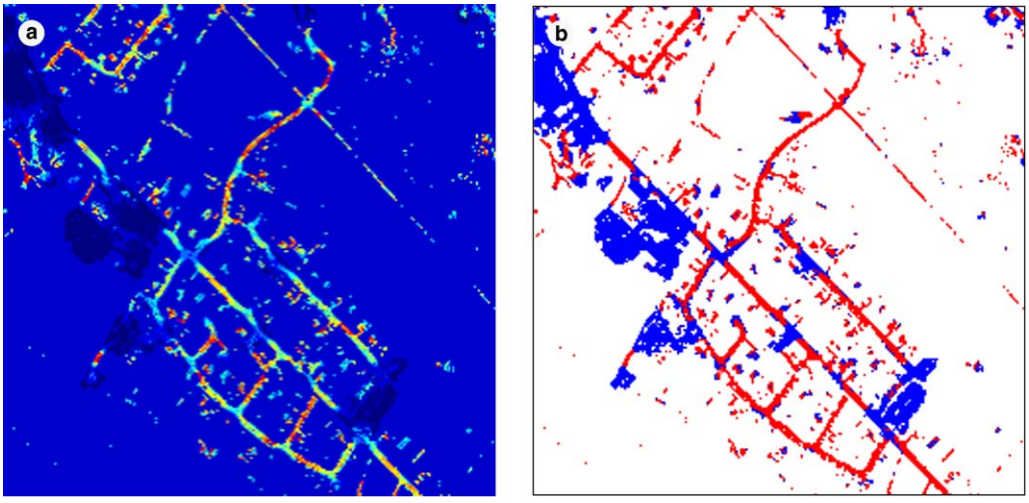

Fig. 11. Road membership (a) of the image shown in Fig. 2; (b) output after thresholding (a) at 0.1. White: non-road pixels, red: road pixels, blue: parking lots/buildings pixels.

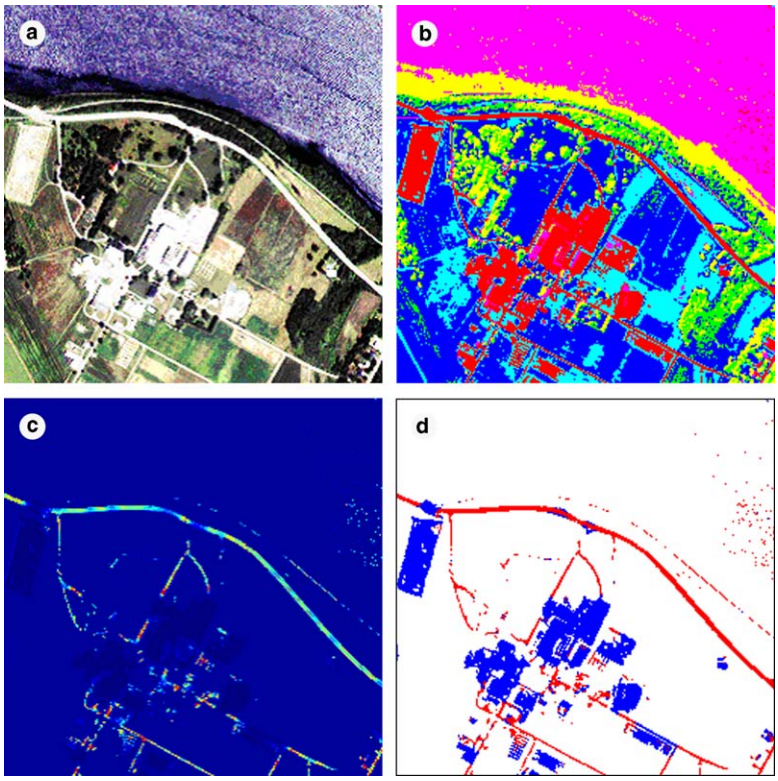

Fig. 12. Result from another Ikonos MS true color composite ortho-image (a), (b) classification result (the identified road cluster shown as red), (c) road membership, (d) separation of roads (in red) and parking lots/buildings and crops (in blue).

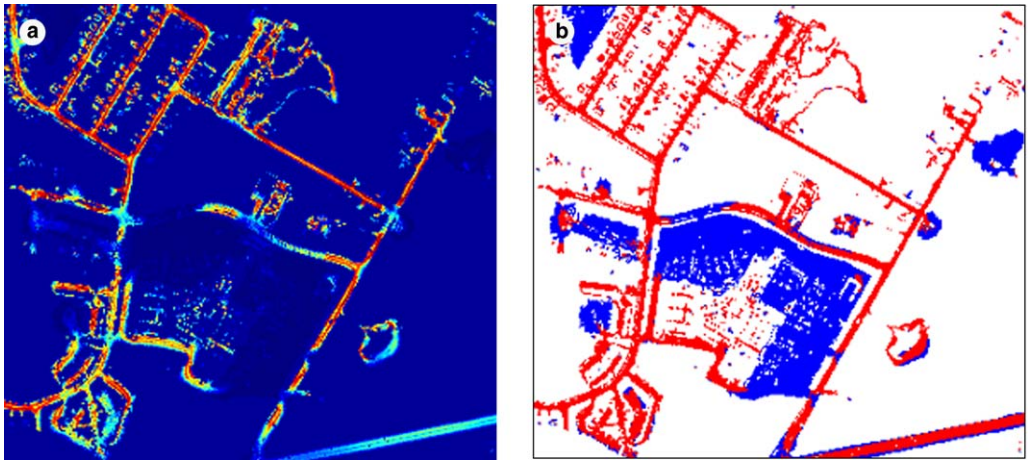

Fig. 13. Road membership (a) and after thresholding (b) of the Quickbird MS ortho-image shown in Fig. 4. In (b) white: non-road pixels, red: road pixels, blue: parking lots/buildings pixels.

Table 3
Evaluation

Test image	Overall accuracy	Kappa statistics			
		Kappa	Variance	z-Value	p-Value
Ikonos MS1 (Fig. 11)	0.70	0.40	0.00007	48.6083	<0.00001
Ikonos MS2 (Fig. 12)	0.84	0.67	0.00004	99.5231	<0.00001
Ikonos MS3	0.76	0.51	0.00008	58.3243	<0.00001
Quickbird MS (Fig. 13)	0.79	0.56	0.00002	128.3495	<0.00001

6. Conclusions

Due to the poor image classification accuracy, little research work has been done in road extraction from multi-spectral imagery. This paper proposed a new road identification approach which integrates a traditional unsupervised classification, a fuzzy logic classification and the angular texture signature. A number of shape descriptors are proposed for the angular texture signature and have been used successfully to separate road pixels from parking lots/buildings. Substantial experiments have shown that the proposed methodology is robust and can be applied to improve the image classification quality for the purpose of feature extraction.

We are currently working on reducing the misclassification of the roads that are closely adjacent to parking lots/buildings and those within a major road intersection. Applying the proposed approach to aerial color imagery and other very high resolution ($\leqslant$1 m) multi-spectral imagery including pan-sharpened imagery will also be included in our future work.

Acknowledgements

We would like to acknowledge the Canadian NCE GEOIDE research program for their financial support of the project "Automating photogrammetric processing and data fusion of very high resolution satellite imagery with LIDAR, iFSAR and maps for fast, low cost and precise 3D urban mapping" and the City of Fredericton, NB, Canada for providing the satellite images. We also thank two anonymous reviewers whose comments improved the quality of the original manuscript.

References

Amini, J., Saradjian, M.R., Blais, J.A.R., Lucas, C., Azizi, A., 2002. Automatic road-side extraction from large scale imagemaps. Int. J. Appl. Earth Observ. Geoinf. 4, 95–107.

Baltsavias, E.P., 2004. Objection extraction and revision by image analysis using existing geodata and knowledge: Current status and steps towards operational systems. ISPRS J. Photogr. Remote Sensing 58, 129–151.

Comaniciu, D., Meer, P., 2002. Mean shift: A robust approach toward feature space analysis. IEEE Trans. Pattern Anal. Machine Intell. 24, 603–619.

Congalton, R.G., Green, K., 1999. Assessing the Accuracy of Remotely Sensed Data: Principles and Practices. Lewis Publishers, 137 p.

Doucette, P., Agouris, P., Musavi, M., Stefanidis, A., 1999. Automated extraction of linear features from aerial imagery using Kohonen learning and GIS data. In: Agouris, P., Stefanidis, A. (Eds.), Integrated Spatial Databases: Digital Images and GIS, Lecture Notes in Computer Science, vol. 1737. Springer-Verlag, Berlin Heidelberg, pp. 20–33.

Doucette, P., Agouris, P., Stefanidis, A., Musavi, M., 2001. Self-organised clustering for road extraction in classified imagery. ISPRS J. Photogr. Remote Sensing 55, 347–358.

Doucette, P., Agouris, P., Stefanidis, A., 2004. Automated road extraction from high resolution multispectral imagery. Photogr. Eng. Remote Sensing 70 (12), 1405–1416.

Gao, J., Wu, L., 2004. Automatic extraction of road networks in urban areas from IKONOS imagery based on spatial reasoning. In: Proc. XX-th ISPRS Congress, Istanbul, Turkey, July 12–23, 2004.

Gardner, M.E., Roberts, D.A., Funk, C., Noronha, V., 2001. Road extraction from AVIRIS using spectral mixture and Q-tree filter techniques. In: Proc. AVIRIS Airborne Geoscience Workshop, 27 February–March, Pasadena, California, URL: ftp://popo.jpl.nasa.gov/pub/docs/workshops/01_docs/toc.html (last date accessed: April 20, 2005).

Gibson, L., 2003. Finding road networks in Ikonos satellite imagery. In: Proc. ASPRS 2003 Conf. Anchorage, Alaska, May 5–9, 2003.

Gonzalez, R.C., Woods, R.E., 2002. Digital Image Processing, second ed. Prentice Hall, Upper Saddle River, NJ.

Haverkamp, D., 2002. Extracting straight road structure in urban environments using IKONOS satellite imagery. Opt. Eng. 41 (9), 2107–2110.

Heijden, F.V.D, 1994. Image Based Measurement Systems: Object Recognition and Parameter Estimation. John Wiley and Sons Ltd., Baffins Lane, Chichester.

Hu, X., Tao, C.V., Hu, Y., 2004. Automatic road extraction from dense urban area by integrated processing of high resolution imagery and lidar data. In: Proc. ISPRS XXth Congress, Istanbul, Turkey, July 12–23, 2004.

Mena, J.B., 2003. State of the art on automatic road extraction for GIS update: A novel classification. Pattern Recognition Lett. 24, 3037–3058.

Mena, J.B., Malpica, J.A., 2005. An automatic method for road extraction in rural and semi-urban areas starting from high resolution satellite imagery. Pattern Recognition Lett. 26 (9), 1201–1220.

Quackenbush, L.J., 2004. A review of techniques for extracting linear features from imagery. Photogr. Eng. Remote Sensing 70 (12), 1383–1392.

Song, M., Civco, D., 2004. Road extraction using SVM and image segmentation. Photogr. Eng. Remote Sensing 70 (12), 1365–1371.

Tarku, K., Bretschneider, T.R., Leedham, C.G., 2004. Unsupervised detection of roads in high resolution panchromatic satellite images. In: Proc. Internat. Workshop Advanced Image Technology (IWAIT-2004), pp. 15–19.

Zhang, Y., Wang, R., 2004. Multi-resolution and multi-spectral image fusion for urban object extraction. In: Proc. ISPRS XXth Congress, Istanbul, Turkey, July 12–23, 2004.